Arabian Journal of Chemistry (2010) 3, 233–242

King Saud University

Arabian Journal of Chemistry

www.ksu.edu.sa
www.sciencedirect.com

ORIGINAL ARTICLE

Corrosion inhibition of copper in chloride media by 2-mercapto-4-(*p*-methoxyphenyl)-6-oxo-1,6-dihydropyrimidine-5-carbonitrile: Electrochemical and theoretical study

N.A. Al-Mobarak [a], K.F. Khaled [b,c,*], Mohamed N.H. Hamed [d], K.M. Abdel-Azim [b], N.S. Abdelshafi [b]

[a] *Faculty of Science, Chemistry Department, Princess Nora Bint Abdulrahman University, Riyadh, Saudi Arabia*
[b] *Electrochemistry Research Laboratory, Chemistry Department, Faculty of Education, Ain Shams University, Roxy, Cairo, Egypt*
[c] *Materials and Corrosion Laboratory, Chemistry Department, Faculty of Science, Taif University, Taif, Hawiya 888, Saudi Arabia*
[d] *Ain Shams University, Faculty of Education, Chemistry Department, Roxy, Cairo, Egypt*

Received 4 May 2010; accepted 8 June 2010
Available online 19 June 2010

KEYWORDS

Copper;
EIS;
EFM;
Quantum chemical calculation;
Molecular modeling

Abstract Electrochemical frequency modulation (EFM), electrochemical impedance spectroscopy (EIS) and potentiodynamic polarization have been used to investigate the inhibition effect of a new pyrimidine heterocyclic derivative, namely 2-mercapto-4-(*p*-methoxyphenyl)-6-oxo-1,6-dihydropyrimidine-5-carbonitrile (MPD) on copper corrosion in 3.5% NaCl solutions at 25 ± 1 °C. The electrochemical investigations showed that MPD gives sufficient inhibition against copper corrosion in 3.5% NaCl solutions. Potentiodynamic polarization measurements have shown that the MPD inhibit both the cathodic and anodic processes and thus it classified as mixed-type inhibitor. EIS measurements indicate that the values of constant phase elements (CPEs) tend to decrease and both charge-transfer resistance and inhibition efficiency tend to increase by increasing the inhibitor concentration. Electrochemical kinetic parameters obtained using EFM methods were comparable with that calculated from traditional measurements (EIS and potentiodynamic polarization). Molecular

* Corresponding author at: Electrochemistry Research Laboratory, Chemistry Department, Faculty of Education, Ain Shams University, Roxy, Cairo, Egypt.
E-mail address: khaledrice2003@yahoo.com (K.F. Khaled).

doi:10.1016/j.arabjc.2010.06.007

Production and hosting by Elsevier

simulation technique was used to investigate the adsorption configuration of MPD on copper surface. Number of electrons transferred from MPD to the copper surface was calculated by semi-empirical quantum chemical calculations.

1. Introduction

Copper and its alloys are industrial materials with a wide variety of applications due to electrical, thermal, mechanical and corrosion resistance properties. However, in the presence of oxygen, chlorides, sulphates or nitrates ions, they are exposed to localized corrosion (Vera et al., 1995; Rosales et al., 1999; Cantor et al., 2006). It is widely used in many applications in electronic industries and communications as a conductor in electrical power lines, pipelines for domestic and industrial water utilities including sea water, heat conductors, heat exchangers, etc. Therefore, corrosion of copper and its inhibition in a wide variety of media, particularly when they contain chloride ions, have attracted the attention of many investigators (Hoepner and Lattemann, 2003; Sherif and Park, 2005; Qu et al., 2005; Singh et al., 2003; Bellakhal and Dachraoui, 2004; Lee and Nobe, 1986; Wang et al., 2004; Kendig and Jeanjaquet, 2002).

The corrosion of copper and its alloys depends to a great extent on the composition of the electrolyte in contact with the metal surface. The process involves copper dissolution at local anodic sites and electrochemical reduction of some species such as oxygen at cathodic areas. In chloride solutions, the first step of the anodic dissolution is the formation of complex $CuCl_2^-$. In addition, it was found that during anodic polarization, there is always equilibrium between a thin layer of CuCl and a dense layer of dissolved $CuCl_2^-$ (Crousier et al., 1988). In natural fresh water, protecting coatings, such as Cu_2O and $Cu(OH)_2$ are formed on copper. These layers influence electrochemical processes at copper electrodes (Bertocci and Turner, 1974; Van Muydler, 1981; Speckmann and Strehblow, 1984).

The role of Cl^- ions in copper corrosion in NaCl centered around (i) a competitive adsorption with OH^- on the available Cu surface, thus creating sites that are more liable for electrochemical dissolution, and (ii) competition with OH^- attached to Cu(II) ions in a soluble intermediate stage, thus enhancing film rupture through dissolution (Cicileo et al., 1998).

The inhibition action of certain organic compounds on metallic corrosion processes has been extensively studied in recent years (Granese et al., 1992; Cicileo et al., 1995; Mansfeld and Wang, 1995; McMahon and Harrop, 1995; Brunoro et al., 1975; Raicheva et al., 1980). There is an agreement of some stages participating in the overall inhibition process, particularly with respect to the mechanism in which inhibition occurs.

Currently, research in copper corrosion is oriented to the development an effective and safe corrosion inhibitors in order to reduce the use of chromates (Mansfeld and Wang, 1995; McMahon and Harrop, 1995; Saleh et al., 1983). In addition heterocyclic organic compounds have generally been used as corrosion inhibitors due to their high inhibition efficiency.

In this study we have investigated the ability of 2-mercapto-4-(*p*-methoxyphenyl)-6-oxo-1,6-dihydropyrimidine-5-carbonitrile (MPD) to inhibit copper corrosion in 3.5% NaCl solution. Electrochemical methods, quantum chemical calculations and molecular dynamic simulations were used to study the interaction between MPD and the copper surface in 3.5% NaCl.

2. Experimental

In this study a new pyrimidine heterocyclic derivative, namely 2-mercapto-4-(*p*-methoxyphenyl)-6-oxo-1,6-dihydropyrimidine-5-carbonitrile (MPD) was prepared in our laboratory where a mixture of 2-cyano-3-(*p*-methoxyphenyl) prop-2-enoate (0.01 mol), thiourea (0.01 mol), anhydrous K_2CO_3 (0.03 mol) in ethanol (30 ml) was heated under reflux for 3 h. The precipitate obtained was washed with water and crystallized from ethanol to give MPD; its structure was confirmed with different spectroscopic techniques (Ram et al., 1984) and presented below:

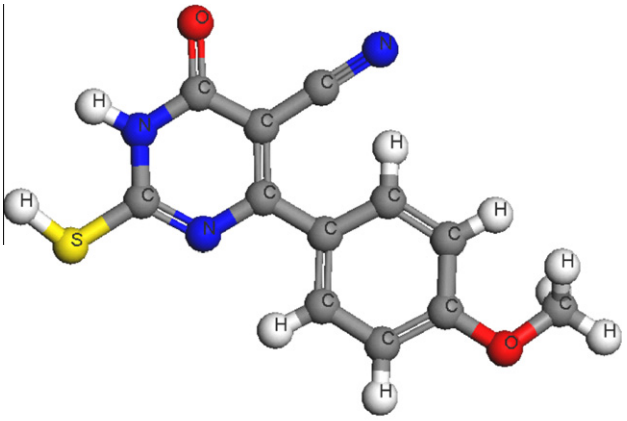

2-Mercapto-4-(p-methoxyPhenyl)-6-oxo-1,6-dihydropyrimidine-5-carbonitrile (MPD)

The MPD is added to the 3.5% NaCl at concentrations of 5×10^{-5}, 10^{-4}, 5×10^{-4} and 10^{-3} M.

Cylindrical rods of copper specimens obtained from Johnson Mattey (Puratronic, 99.999%) were mounted in Teflon. An epoxy resin was used to fill the space between Teflon and copper electrode. The circular cross sectional area of the copper rod exposed to the corrosive medium, used in electrochemical measurements, was (0.28 cm^2).

The electrochemical measurements were performed in a typical three-compartment glass cell consisted of the copper specimen as working electrode (WE), platinum counter electrode (CE), and a saturated calomel electrode (SCE) as the reference electrode. The counter electrode was separated from the working electrode compartment by fritted glass. The reference electrode was connected to a Luggin capillary to minimize IR drop. Solutions were prepared from bidistilled water of resistivity 13 MΩ cm, the copper electrode was abraded with different grit emery papers up to 4/0 grit size, cleaned with acetone, washed with double-distilled water and finally dried.

Tafel polarization curves were obtained by changing the electrode potential automatically from −800 to +300 mV_{SCE} at open circuit potential with scan rate of 1.0 mV s^{-1}. Impedance measurements were carried out in frequency range from 100 kHz to 40 mHz with an amplitude of 10 mV peak-to-peak using ac signals at open circuit potential. Electrochemical frequency modulation, EFM, was carried out using two frequencies 2 Hz and 5 Hz. The base frequency was 1 Hz, so the waveform repeats after 1 s. The higher frequency must be at least two times the lower one. The higher frequency must also be sufficiently slow that the charging of the double layer does not contribute to the current response. Often, 10 Hz is a reasonable limit.

The electrode potential was allowed to stabilize 60 min before starting the measurements. All experiments were conducted at 25 ± 1 °C. Measurements were performed using Gamry Instrument Potentiostat/Galvanostat/ZRA. This includes a Gamry Framework system based on the ESA400, Gamry applications that include dc105 for dc corrosion measurements, EIS300 for electrochemical impedance spectroscopy and EFM 140 for electrochemical frequency modulation measurements along with a computer for collecting data. Echem Analyst 5.58 software was used for plotting, graphing and fitting data.

3. Computational details

The correlation between theoretically calculated properties and experimentally determined inhibition efficiencies has been studied successfully for uniform corrosion (Vosta and Eliasek, 1971; Chakrabarti, 1984; Abdul-Ahad and Al-Madfai, 1989; Growcock, 1989; Costa and Lluch, 1984; Kutej et al., 1995; Lukovits et al., 1995, 1999; Awad et al., 1997; Bereket et al., 2001, 2002). Several theoretical parameters includes the electronic properties of inhibitors, effects of the frontier molecular orbital energies, the differences between lowest unoccupied molecular orbital (LUMO) and highest occupied molecular orbital (HOMO) energies ($E_L - E_H$), electronic charges on reactive centers, dipole moments and conformation of molecules have been investigated by semi-empirical methods. First step for calculating the theoretical parameters of the studied molecule is the geometry optimization process which is carried out using an iterative process, in which the atomic coordinates are adjusted until the total energy of a structure is minimized, i.e., it corresponds to a local minimum in the potential energy surface. Interaction between MPD and Cu (1 1 1) surface was carried out in a simulation box (15.45 Å × 15.45 Å × 43.61 Å) with periodic boundary conditions to model a representative part of the interface devoid of any arbitrary boundary effects. The Cu (1 1 1) was first built and relaxed by minimizing its energy using molecular mechanics, then the surface area of Cu (1 1 1) was increased and its periodicity is changed by constructing a super cell, and then a vacuum slab with 30 Å thicknesses was built on the Cu (1 1 1) surface. The number of layers in the structure was chosen so that the depth of the surface is greater than the non-bond cutoff used in calculation. Using 6 layers of Cu atoms gives a sufficient depth that the inhibitor molecules will only be involved in non-bond interactions with Cu atoms in the layers of the surface, without increasing the calculation time unreasonably. This structure then converted to have 3D periodicity. After minimizing the Cu (1 1 1) surface and MPD molecules, the corrosion system will be built by layer builder to place the inhibitor molecules on Cu (1 1 1) surface, and the behaviour of the MPD molecules on the Cu (1 1 1) surface were simulated using the condensed phase optimized molecular potentials for atomistic simulation studies force field (COMPASS).

The Discover molecular dynamics module in Materials Studio 5.0 software from Accelrys Inc. (Barriga et al., 2007) have been used in performing the molecular dynamic simulations which described elsewhere (Khaled, 2009). The interaction energy, $E_{Cu\text{-}inhibitor}$, of the Cu (1 1 1) surface with MPD was calculated according to the following Eq. (1):

$$E_{Cu\text{-}inhibitor} = E_{complex} - (E_{Cu\text{-}surface} + E_{inhibitor}) \quad (1)$$

where $E_{complex}$ is the total energy of the Cu (1 1 1) surface together with the adsorbed inhibitor molecule, $E_{Cu\text{-}surface}$ and $E_{inhibitor}$ are the total energy of the Cu (1 1 1) surface and free inhibitor molecule, respectively. The binding energy between MPD and Cu (1 1 1) surfaces was the negative value of the interaction energy (Mineva et al., 2001), as follow:

$$E_{binding} = -E_{Cu\text{-}inhibitor}. \quad (2)$$

4. Results and discussion

4.1. Experimental measurements

Several traditional corrosion techniques implied to study the corrosion inhibition of copper by MPD in 3.5% NaCl solutions to evaluate the electrochemical kinetic parameters obtained by using electrochemical frequency modulation as a new technique that can be used to calculate the corrosion rate of a metal without a prior knowledge of Tafel slopes. Potentiodynamic polarization and electrochemical impedance spectroscopy, EIS measurements are used to calculate the inhibition efficiency as well as other corrosion kinetic parameters.

4.1.1. Electrochemical frequency modulation, EFM

The result of EFM experiments is a spectrum of current response as a function of frequency. The spectrum is called the 'intermodulation spectrum'. Fig. 1 shows the corresponding current response in the intermodulation spectrum for copper in aerated 3.5% NaCl solutions at 25 ± 1 °C.

Electrochemical kinetic parameters calculated from EFM for copper in 3.5% NaCl are listed in Table 1 and calculated using the following Eqs. (3–7):

$$i_{corr} = \frac{i_\omega^2}{\sqrt{48(2i_\omega i_{3\omega} - i_{2\omega})}} \quad (3)$$

$$\beta_a = \frac{i_\omega U_o}{2i_{2\omega} + 2\sqrt{3}\sqrt{2i_{3\omega}i_\omega - i_{2\omega}^2}} \quad (4)$$

$$\beta_c = \frac{i_\omega U_o}{2\sqrt{3}\sqrt{2i_{3\omega}i_\omega - i_{2\omega}^2 - 2i_{2\omega}}} \quad (5)$$

$$\text{Causality factor (2)} = \frac{i_{\omega_2 \pm \omega_1}}{i_{2\omega_1}} = 2.0 \quad (6)$$

$$\text{Causality factor (3)} = \frac{i_{2\omega_2 \pm \omega_1}}{i_{3\omega_1}} = 3.0 \quad (7)$$

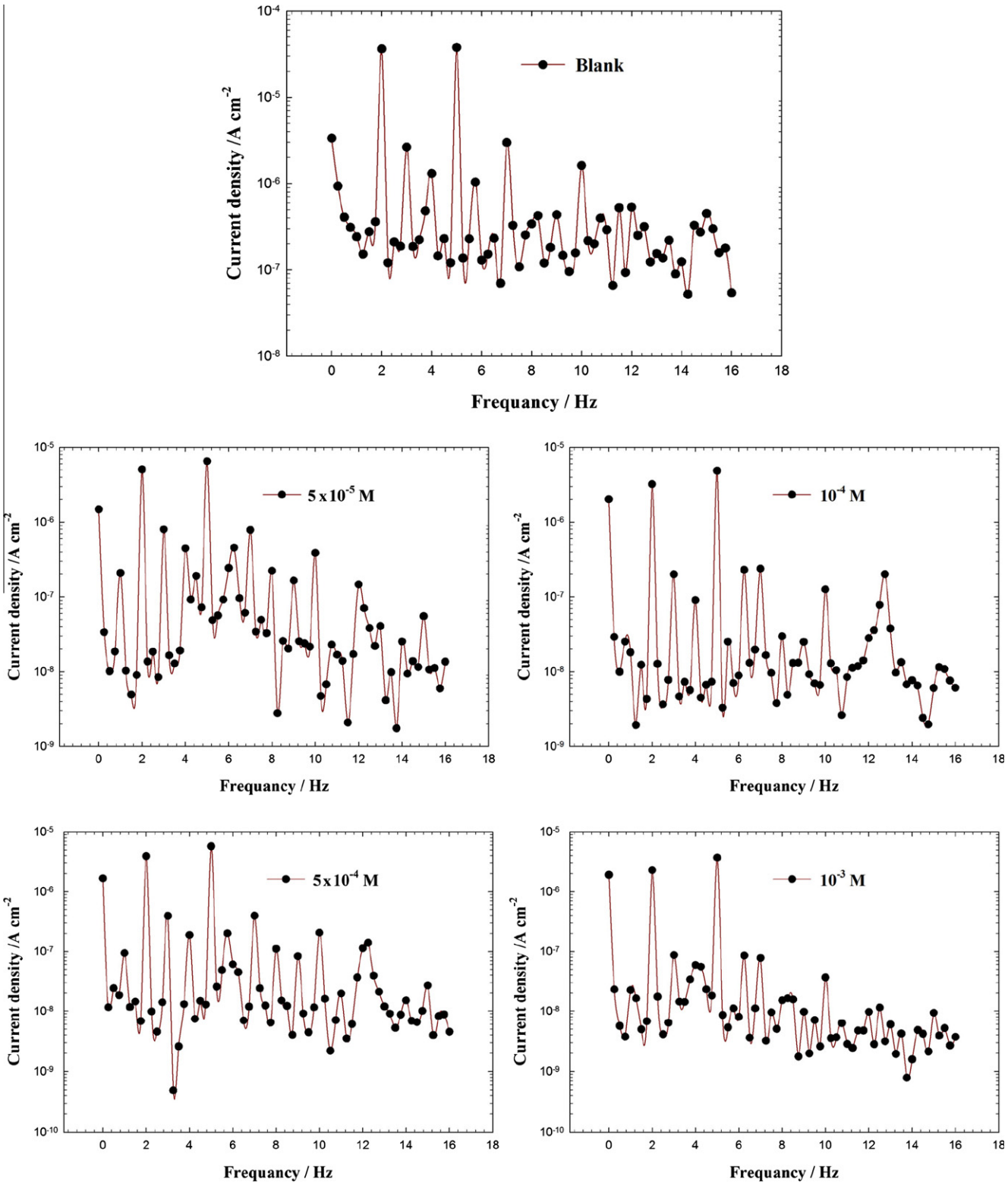

Figure 1 Intermodulation spectra recorded for copper electrode in 3.5% NaCl solutions in the absence and presence of various concentrations of MPD at 25 ± 1 °C.

where i is the instantaneous current density at the working copper electrode measured at frequency ω and U_o is the amplitude of the sine wave distortion.

Table 1 shows the corrosion kinetic parameters such as inhibition efficiency (E_{EFM}%), corrosion current density ($\mu A\ cm^{-2}$), Tafel constants (β_a, β_c) and causality factors (CF-2, CF-3) at different concentration of MPD derivative in 3.5% NaCl at 25 ± 1 °C.

It is obvious from Table 1 that, the corrosion current densities decrease by increasing the concentrations of these

Table 1 Electrochemical kinetic parameters obtained by EFM technique for copper in 3.5% NaCl with various concentrations of MPD at 25 ± 1 °C.

	Concentration (M)	i_{corr} (μA cm^{-2})	β_a (mV dec^{-1})	β_c (mV dec^{-1})	C.R. (mpy)	E_{EFM}(%)	CF-2	CF-3
	Blank	71.75	71.76	119.1	117.1		1.9	1.4
MPD	5×10^{-5}	7.44	52.73	97.30	12.80	89.63	1.8	2.5
	10^{-4}	6.89	70.60	108.0	11.18	90.40	1.8	1.6
	5×10^{-4}	4.35	126.80	219.3	9.45	93.94	2.0	2.2
	10^{-3}	3.47	149.50	200.2	8.25	95.16	1.7	3.01

compounds. The inhibition efficiencies increase by increasing MPD concentrations. The causality factors in Table 1 are very close to the theoretical values which according to the EFM theory (Khaled, 2008) should guarantee the validity of Tafel slopes and corrosion current densities. Inhibition efficiency (E_{EFM}%) depicted in Table 1 calculated from the following Eq. (8):

$$E_{EFM}\% = \left(1 - \frac{i_{corr}}{i^{o}_{corr}}\right) \times 100 \quad (8)$$

where i^{o}_{corr} and i_{corr} are corrosion current density in the absence and presence of MPD derivative, respectively.

It is clear from Table 1 that the corrosion current densities decrease with increase in MPD concentrations. Values of the causality factors in Table 1 indicate that the measured data are of good quality. The standard values for CF-2 and CF-3 are 2.0 and 3.0, respectively. The causality factors are calculated from the frequency spectrum of the current response. If the causality factors differ significantly from the theoretical values of 2.0 and 3.0, then it can be deduced that the measurements are influenced by noise. If the causality factors are approximately equal to the predicted values of 2.0 and 3.0, i.e. there is a causal relationship between the perturbation signal and the response signal. Then the data are assumed to be reliable (Bosch et al., 2001).

The great strength of the EFM is the causality factors which serve as an internal check on the validity of the EFM measurement (Bosch et al., 2001; Abdel-Rehim et al., 2006). With the causality factors the experimental EFM data can be verified. The standard values for CF-2 and CF-3 are 2.0 and 3.0, respectively. The deviation of causality factors from their ideal values might due to that the perturbation amplitude was too small or that the resolution of the frequency spectrum is not high enough also another possible explanation that the inhibitor is not performing very well. In an attempt to evaluate the EFM technique as an effective corrosion monitoring technique, several traditional techniques implied to study the corrosion inhibition of copper by MPD in 3.5% NaCl media. Both EIS and potentiodynamic polarization techniques are used to calculate the inhibition efficiency as well as other corrosion kinetic parameters.

4.1.2. Impedance measurements

The corrosion behaviour of copper in 3.5% NaCl in absence and presence of MPD investigated by EIS after immersion for 1 h at 25 ± 1 °C. Nyquist plots of copper in uninhibited and inhibited sodium chloride solutions containing various concentrations of MPD are presented in Fig. 2.

The shape of the impedance diagrams of copper in 3.5% NaCl is similar to those found in the literature (Khaled, 2008). The presence of MPD increases the impedance but does not change the other aspects of corrosion mechanism occurred due to its addition. Symbols in Fig. 2 represent the measured data and solid lines represent the fitting data obtained using

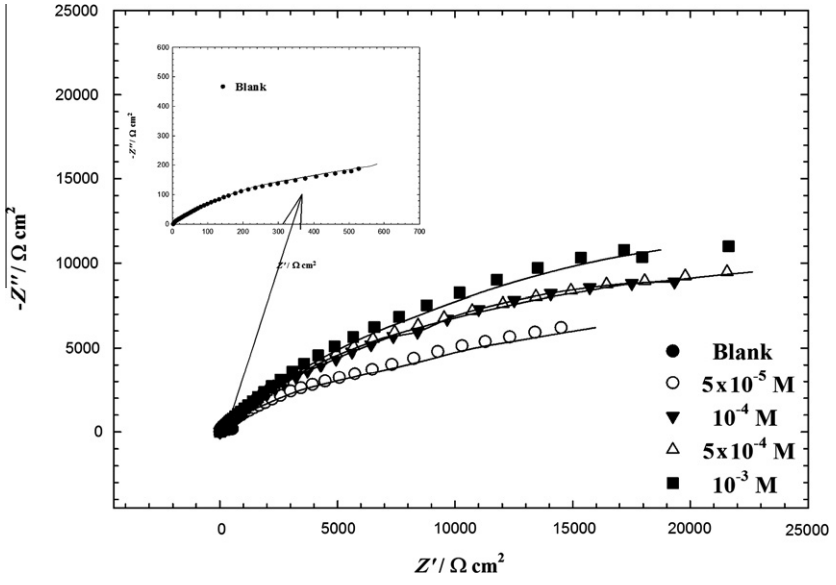

Figure 2 Nyquist plots for copper in 3.5% NaCl solutions in the absence and presence of various concentrations of MPD at 25 ± 1 °C.

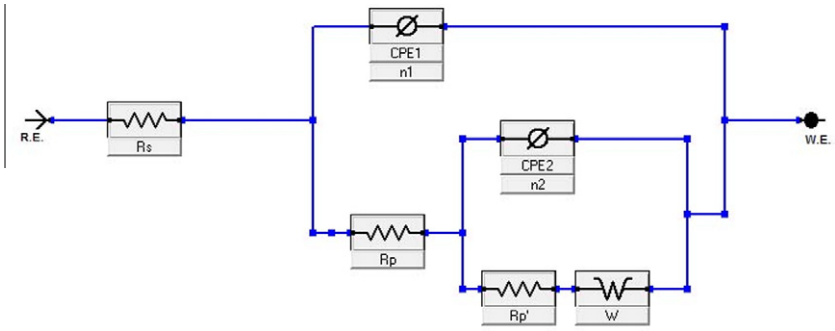

Figure 3 Equivalent circuits used to model impedance data for copper in 3.5% NaCl solutions in the absence and presence of various concentrations of MPD at 25 ± 1 °C.

the equivalent circuit (Sherif and Park, 2006) presented in Fig. 3. The parameters obtained by fitting the experimental data using the equivalent circuit, and the calculated inhibition efficiencies are listed in Table 2, where R_s represents the solution resistance, R_p is the polarization resistance and can be defined also as the charge-transfer resistance, CPE_1 and CPE_2 are constant phase elements (CPEs), R'_p is another polarization resistance and W, is the Warburg impedance. The Nyquist plots presented in Fig. 2 clearly demonstrate that the shapes of these plots for inhibited copper electrode are not substantially different from those of uninhibited electrode. Addition of MPD molecules increases the impedance but does not change other aspects of the electrode behaviour. Nyquist spectra presented in Fig. 2 are modeled using an equivalent circuit model similar to the one proposed by several authors (Juttner et al., 1988, 1986).

The impedance spectra obtained for copper in 3.5% NaCl contains depressed semicircle with the center under the real axis, such behaviour is characteristic for solid electrodes and often referred to as frequency dispersion and attributed to the roughness and other inhomogenities of the solid electrode (Ma et al., 2002; Pajkossy, 1994).

Parameters derived from EIS measurements and inhibition efficiency is given in Table 2. Addition of MPD increases the values of R_p and R'_p and lowers the values of CPE_1 and CPE_2 and this effect is seen to be increased as the concentrations of MPD increase. The constant phase elements (CPEs) with their n values $1 > n > 0$ represent double layer capacitors with some pores (Sherif and Park, 2006). The CPEs decrease upon increase in MPD concentrations, which are expected to cover the charged surfaces and reducing the capacitive effects.

This decrease in (CPE) results from a decrease in local dielectric constant and/or an increase in the thickness of the double layer, suggested that MPD molecules inhibit the copper corrosion by adsorption at the copper/NaCl interface The semicircles at high frequencies in Fig. 2 are generally associated with the relaxation of electrical double layer capacitors and the diameters of the high frequency semicircles can be considered as the charge-transfer resistance ($R_{ct} = R_p$) Ma et al., 2002. Therefore, the inhibition efficiency, $\eta\%$ of MPD for the copper electrode can be calculated from the charge-transfer resistance as follows (Ma et al., 2002):

$$\eta\% = \left(1 - \frac{R_p^o}{R_p}\right) \times 100 \quad (9)$$

where R_p^o and R_p are the polarization resistances for uninhibited and inhibited solutions, respectively. The CPEs are almost like Warburg impedance with their n values close to 0.5 in presence of MPD (Sherif and Park, 2006), which suggests that the electron transfer reaction corresponding to the second semicircle takes place through the surface layer and limits the mass transport (Warburg). The presence of the Warburg (W) impedance in the circuit also confirms that the mass transport is limited by the surface passive film.

4.1.3. Potentiodynamic polarization measurements

Measurements of current-potential values under carefully controlled conditions can yield information on corrosion rates, coatings and films, passivity, pitting tendencies and other important phenomena.

When a copper specimen is immersed in 3.5% NaCl, both reduction and oxidation processes occur on its surface. Typically, the copper specimen oxidizes (corrodes) and the oxygen is reduced. The cathodic reaction of copper in aerated sodium chloride solutions is well known to be the oxygen reduction (Vera et al., 1995; Sherif, 2006)

Table 2 Electrochemical parameters calculated from EIS measurements on copper electrode in 3.5% NaCl solutions without and with various concentrations of MPD derivatives 25 ± 1 °C using equivalent circuit presented in Fig. 3.

Inhibitor		R_s (Ω cm^2)	R_p (Ω cm^2)	CPE_1 ($\mu\Omega^{-1}$ cm^{-2} S^{n_1})	n_1	R'_p (Ω cm^2)	CPE_2 ($\mu\Omega^{-1}$ cm^{-2} S^{n_2})	n_2	W ($\mu\Omega^{-1}$ cm^{-2} S$^{1/2}$)	η (%)
	Blank	113	733	1.3	0.89	6.1	13.5	0.52	20.3	
MPD	5×10^{-5}	97.3	4662	0.4	0.79	15.6	4.5	0.53	6.2	85.1
	10^{-4}	89.4	6154	0.34	0.91	17.6	3.2	0.46	3.2	89.2
	5×10^{-4}	99.3	9302	0.27	0.76	19.8	2.3	0.61	1.5	93.3
	10^{-3}	89.7	12572	0.04	0.89	20.9	1.1	0.43	0.8	96.2

$$O_2 + 2H_2O + 4e^- \rightarrow 4OH^- \quad (10)$$

Any corrosion processes that occur are usually a result of anodic currents. When a copper specimen is not connected to any instrumentation as it would be "in service" the specimen assumes a potential (relative to a reference electrode) termed the corrosion potential, E_{corr}. The corrosion potential, E_{corr} can be defined as the potential at which the rate of oxidation is exactly equal to the rate of reduction (Basics of corrosion measurements, 1982).

The potentiodynamic polarization curves recorded for the copper electrode in the absence and presence of MPD are presented in Fig. 4. As can be seen from Fig. 4 that the anodic branch of Cu in NaCl solutions in the absence and the presence of MPD molecules shows a three distinct regions; firstly, increasing the current from the Tafel region at lower overpotentials, which extending to the peak current density due to the dissolution of copper metal to Cu^+

$$Cu \rightarrow Cu^+ + e^- \quad (11)$$

Secondly, the region of decreasing currents until a minimum is reached due to the formation of CuCl

$$Cu^+ + Cl^- \rightarrow CuCl \quad (12)$$

And finally the region of sudden increase in current density leading to a limiting value as a result of $CuCl_2^-$ formation which is responsible on the dissolution of Cu

$$CuCl + C^- \rightarrow CuCl_2^- \quad (13)$$

It is also seen from Fig. 4 that increasing the MPD concentrations, decreases the cathodic, anodic and corrosion currents (i_{corr}) and consequently the corrosion rates.

It has been shown that in the Tafel extrapolation method, the use of both the anodic and cathodic Tafel regions is undoubtedly preferred over the use of only one Tafel region (McCafferty, 2005). However, the corrosion rate can also be determined by Tafel extrapolation of either the cathodic or anodic polarization curve alone. If only one polarization curve is used, it is generally the cathodic curve which usually produces a longer and better defined Tafel region. Anodic polarization may sometimes produce concentration effects, due to passivation and dissolution, as well as roughening of the surface which can lead to deviations from Tafel behaviour.

The situation is quite different here; the anodic dissolution of copper in aerated 3.5% NaCl solutions obeys, as previously mentioned, Tafel's law. The anodic curve is, therefore preferred over the cathodic one for evaluation of corrosion currents, i_{corr}, by the Tafel extrapolation method. However, the cathodic polarization curve deviate from the Tafel behaviour, exhibiting a limiting diffusion current, may be due to the reduction of dissolved oxygen. Accordingly, there is a source of error in the numerical values of the cathodic Tafel slopes calculated by the software. For this reason, the values of the

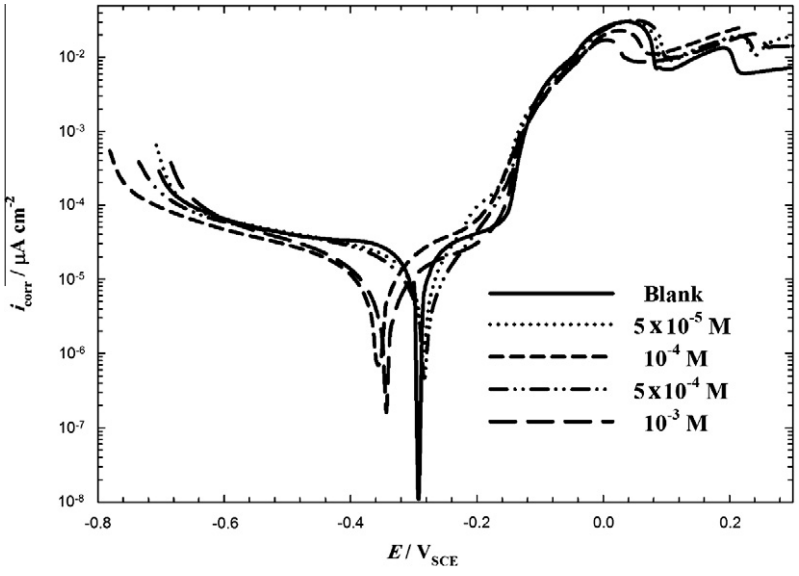

Figure 4 Anodic and cathodic polarization curves for copper in 3.5% NaCl solutions in the absence and presence of various concentrations of MPD at 25 ± 1 °C.

Table 3 Electrochemical kinetic parameters obtained by potentiodynamic technique for copper in 3.5% NaCl without and with various concentrations of MPD at 25 ± 1 °C.

	Concentration (M)	i_{corr} (μA cm^{-2})	$-E_{corr}$ (mV) (SCE)	β_a (mV dec^{-1})	υ_p (%)
MPD	Blank	11.30	293.0	227.0	–
	5×10^{-5}	4.45	285.0	202.4	84.28
	10^{-4}	3.37	356.0	162.2	88.09
	5×10^{-4}	2.23	283.0	177.6	92.12
	10^{-3}	1.65	344.0	191.0	94.17

cathodic Tafel slopes, calculated from the software, are not included here.

Addition of 10^{-3} M of MPD reduces to a great extent the cathodic and anodic currents, i_{corr}. The corresponding electrochemical kinetics parameters such as corrosion potential (E_{corr}), anodic Tafel slopes (β_a) and corrosion current density (i_{corr}), obtained by extrapolation of the Tafel lines are presented in Table 3. The inhibitor efficiency was evaluated from dc measurements using the following Eq. (14) (Hack and Pickering, 1991):

$$\upsilon_p\% = \left(1 - \frac{i_{corr}}{i^{o}_{corr}}\right) \times 100 \quad (14)$$

where i^{o}_{corr} and i_{corr} correspond to uninhibited and inhibited current densities, respectively.

Inspection of Table 3, shows that the addition of different concentration of MPD decreases corrosion current densities and increases the inhibition efficiencies $\upsilon_p\%$.

4.2. Molecular dynamics simulations

In an attempt for understanding the interaction between MPD molecules and copper/copper oxide surface, molecular dynamic simulations study have been performed to simulate the adsorption of MPD on the copper surface. Inspection of molecular structure of MPD shows that it is likely to adsorb on copper surface by sharing the electrons of nitrogen, sulphur, oxygen, phenyl rings and pyrimidine structure with copper. The adsorption progress of MPD on copper surface is investigated by performing molecular mechanics (MM) using MS modeling software. The periodic boundary conditions (PBC) were applied to the simulation cell and described elsewhere (Khaled, 2008). MPD molecule was energy optimized, copper surface was constructed using the amorphous cell module, the whole system was energy optimized and the possibility of MPD adsorption on the copper surface were simulated as in Fig. 5. It could be seen from Fig. 5 that MPD molecule move near to the copper surface, indicating that MPD adsorbed at copper surface. Fig. 5 shows that the adsorption occurred through the nitrogen atoms in MPD. During simulation, both in plane aromatic structures are fluctuating up and down the copper surface while nitrogen atoms are attached all the time to copper surface.

The adsorption density of MPD on the Cu (1 1 1) substrate has been presented in Fig. 6. Therefore, the studied molecules are likely to adsorb on the copper surface to form stable adsorption layers and protect copper from corrosion. The binding energies as well as the adsorption energy were calculated and presented in Table 4.

The parameters presented in Table 4 include total energy, in kcal mol^{-1}, of the substrate–adsorbate configuration. The total energy is defined as the sum of the energies of the adsorbate components, the rigid adsorption energy and the deformation energy. In this study, the substrate energy (copper surface) is

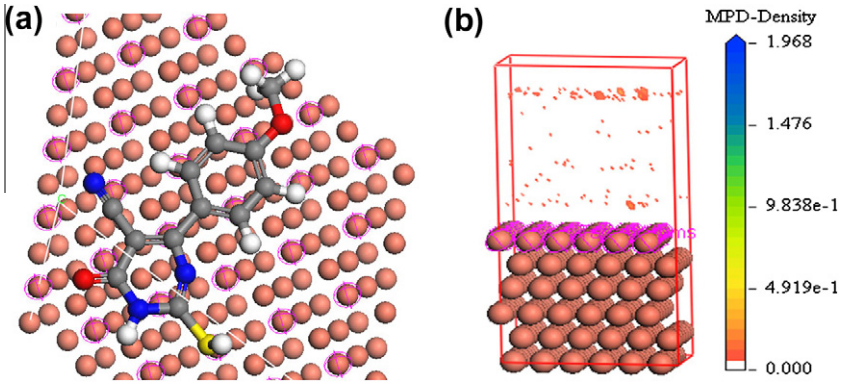

Figure 5 (a) Most suitable configuration for adsorption of MPD on Cu (1 1 1) substrate obtained by adsorption locator module. (b) The adsorption density of MPD on the Cu (1 1 1) substrate.

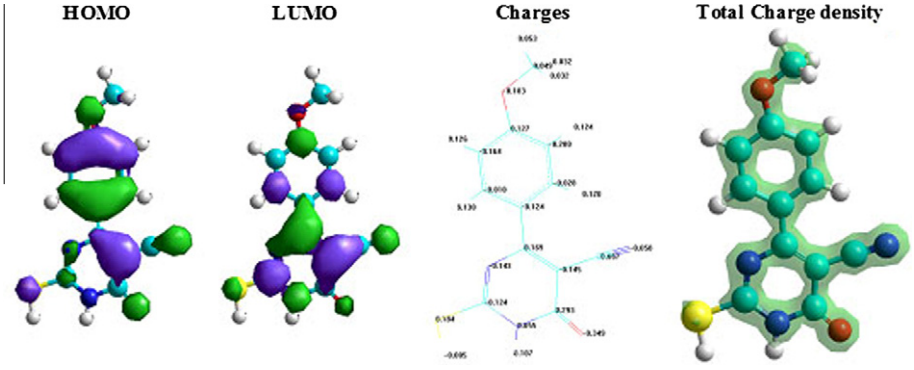

Figure 6 Frontier molecular orbital, charges distribution and electron density plots for MPD.

Table 4 Quantum chemical and molecular dynamics parameters derived for MPD calculated with DFT method in aqueous phase.

Property	Value
Total energy (kcal mol^{-1})	−86061.3
μ (D)	4.3
E_{HOMO} (eV)	−8.4
E_{LUMO} (eV)	−1.46
ΔE (eV)	6.94
$I = -E_{HOMO}$	8.4
$A = -E_{LUMO}$	1.46
$\chi = (I + A)/2$	4.93
$\eta = (I - A)/2$	3.47
$\Delta N = \frac{\chi_{Cu} - \chi_{inh}}{2(\eta_{Cu} + \eta_{inh})}$	0.06
$E_{Cu\text{-}inhibitor}$ (kcal mol^{-1})	−543.8
$E_{binding}$ (kcal mol^{-1})	543.8
Adsorption energy (kcal mol^{-1})	−436.6
Rigid adsorption energy (kcal mol^{-1})	−78.2
Deformation energy (kcal mol^{-1})	−358.5
dE_{ad}/dN_i (kcal mol^{-1})	−436.6

taken as zero. In addition, adsorption energy in kcal mol^{-1}, reports energy released (or required) when the relaxed adsorbate components (MPD molecule) are adsorbed on the substrate. The adsorption energy is defined as the sum of the rigid adsorption energy and the deformation energy for the adsorbate components. The rigid adsorption energy reports the energy, in kcal mol^{-1}, released (or required) when the unrelaxed adsorbate components (i.e., before the geometry optimization step) are adsorbed on the substrate. The deformation energy reports the energy, in kcal mol^{-1}, released when the adsorbed adsorbate components are relaxed on the substrate surface. Table 4 shows also (dE_{ads}/dNi), which reports the energy, in kcal mol^{-1}, of substrate–adsorbate configurations where one of the adsorbate components has been removed. The binding energy introduced in Table 4 calculated from Eq. (2).

4.2.1. Quantum chemical calculations

The Mulliken atomic charges distributions of MPD molecule as well as the highest occupied molecular orbitals (HOMO) and lowest unoccupied molecular orbital (LUMO) were calculated using Hperchem 8.0.7 software and presented in Fig. 6.

It is confirmed that the more negative the atomic partial charges of the adsorbed centre are, the more easily the atom attracted to the metal surface.

Some of the key quantum chemical parameters were computed using the PM3-SCF method and presented in Table 4. These are mainly the energies of the highest occupied (E_{HOMO}) and lowest unoccupied (E_{LUMO}) molecular orbitals and total energy (E_{tot}). These quantum chemical parameters were obtained after geometric optimization with respect to the all nuclear coordinates.

Frontier orbital theory is useful in predicting adsorption centers of the inhibitor molecules responsible for the interaction with surface metal atoms (Fang and Li, 2002; Bereket et al., 2002). Moreover, the gap between the LUMO and HOMO energy levels of the molecules was another important factor that should be considered. Reportedly, excellent corrosion inhibitors are usually those organic compounds who are not only offer electrons to unoccupied orbital of the metal, but also accept free electrons from the metal (Zhao et al., 2005).

It is well established in the literature that the higher the HOMO energy of the inhibitor, the greater the trend of offering electrons to unoccupied d orbital of the copper ion, and the higher the corrosion inhibition efficiency. In addition, the lower the LUMO energy, the easier the acceptance of electrons from metal surface, as the LUMO–HOMO energy gap decreased and the efficiency of inhibitor improved. Quantum chemical parameters listed in Table 4 reveal that MPD has high HOMO and low LUMO with high energy gap.

The number of transferred electrons (ΔN) was also calculated depending on the quantum chemical method as in the following Eq. (15):

$$\Delta N = \frac{\chi_{Cu} - \chi_{inh}}{2(\eta_{Cu} + \eta_{inh})} \tag{15}$$

where χ_{Cu} and χ_{inh} denote the absolute electronegativity of copper and the MPD molecule, respectively; η_{Cu} and η_{inh} denote the absolute hardness of copper and the inhibitor molecule, respectively. These quantities are related to electron affinity (A) and ionization potential (I) which are useful in their ability to help predict chemical behaviour (Pearson, 1986).

$$\chi = \frac{I + A}{2} \tag{16}$$

$$\eta = \frac{I - A}{2} \tag{17}$$

I and A are related in turn to E_{HOMO} and E_{LUMO}

$$I = -E_{HOMO} \tag{18}$$

$$A = -E_{LUMO} \tag{19}$$

Values of χ and η were calculated by using the values of I and A obtained from quantum chemical calculation. Using a theoretical χ value of 4.48 eV/mol according to Pearsons electronegativity scale and η value of 0 eV/mol for copper (Pearson, 1988), ΔN, is the fraction of electrons transferred from inhibitor to the copper surface, was calculated. Values of ΔN showed inhibition effect resulted from electrons donation. Agreeing with Lukovits's study (Lukovits et al., 2001), if $\Delta N < 3.6$, the inhibition efficiency increased with increasing electron-donating ability at the metal surface. In this study, MPD was the donor of electrons, and the copper oxide surface was the acceptor. MPD was bound to the copper oxide surface, and thus formed inhibitive adsorption layer against corrosion.

The vertical distance, calculated from molecular dynamics, between the flat molecules and copper surface was about 2.1 Å for MPD; this result indicates that the interaction between the MPD molecules and the copper surface is strong enough to inhibit corrosion.

5. Conclusion

The main conclusions of the present study can be summarized as follows.

MPD presents good inhibition efficiency against copper corrosion in 3.5% sodium chloride solutions. Tafel polarization studies have shown that the MPD suppresses both the cathodic and anodic processes and thus it acts as mixed-type inhibitor. EIS measurements indicate that the value of CPEs

tends to decrease and both charge-transfer resistance and inhibition efficiencies tend to increase by increasing the MPD concentration. This result can be attributed to increase of the thickness of the electrical double layer. Electrochemical kinetic parameters obtained from EFM technique are in good agreement with that obtained from traditional electrochemical measurements. Accordingly EFM can be used as a rapid and non destructive technique for corrosion rate measurements without prior knowledge of Tafel constants. Molecular dynamic simulations and quantum chemical calculations are performed to investigate the adsorption behaviour of MPD on copper surface.

Acknowledgement

The authors' gratefully acknowledge the inhibitor preparation carried out by Dr. K. M. El-Mahdy, lecturer of organic chemistry, chemistry department, faculty of education, Ain Shams University, Roxy, Cairo, Egypt.

References

Abdel-Rehim, S.S., Khaled, K.F., Abdel-Shafi, N.S., 2006. Electrochim. Acta 51, 3267.
Abdul-Ahad, P.G., Al-Madfai, S.H.F., 1989. Corrosion 45, 978.
Awad, G.H., Asad, A.N., Abdel Gaber, A.M., Masud, S.S., 1997. Zashchita Metallov 33, 6 (see also p. 565).
Barriga, J., Coto, B., Fernandez, B., 2007. Tribol. Int. 40, 960.
Basics of corrosion measurements, 1982. Application Note No. 1 (EG&G PRISTON APPLIED RESEARCH), P.1.
Bellakhal, N., Dachraoui, M., 2004. Mater. Chem. Phys. 85, 366.
Bereket, G., Ogretir, C., Yurt, A., 2001. J. Mol. Struct. (THEOCHEM) 571, 139.
Bereket, G., Ogretir, C., Hur, E., 2002. J. Mol. Struct. (THEOCHEM) 578, 79.
Bertocci, U., Turner, D., 1974. In: Bard, A.J. (Ed.), Encyclopedia of Electrochemistry of the Elements, vol. II. Marcel Dekker, New York.
Bosch, R.W., Hubrecht, J., Bogaerts, W.F., Syrett, B.C., 2001. Corrosion 57, 60.
Brunoro, G., Trabanelli, G., Zucchi, F., 1975. In: Proceedings of Third European Symp. Corrosion Inhibitors, Ferrara, Italy, p. 443.
Cantor, A., Bushman, J., Glodoski, M., Kiefer, E., Bersch, R., Wallenkamp, H., 2006. Mater. Perfor. 45, 38.
Chakrabarti, A., 1984. Br. Corros. J. 19, 124.
Cicileo, G.P., Rosales, B.M., Vilche, J.R., 1995. In: Proceedings Seventh European Symp. Corrosion Inhibitors, Ferrara, Italy, p. 1011.
Cicileo, G.P., Rosales, B.M., Varela, E., Vilche, J.R., 1998. Corros. Sci. 39, 1915.
Costa, J.M., Lluch, J.M., 1984. Corros. Sci. 24, 929.
Crousier, J., Pardessus, L., Croussier, J.P., 1988. Electrochim. Acta 33, 1039.
Fang, J., Li, J., 2002. J. Mol. Struct. (THEOCHEM) 593, 179.
Granese, S.L., Rosales, B.M., Oviedo, C., Zerbino, J.O., 1992. Corros. Sci. 33, 1439.
Growcock, F.B., 1989. Corrosion 45, 1003.
Hack, H.P., Pickering, H.W., 1991. J. Electrochem. Soc. 138, 690.
Hoepner, T., Lattemann, S., 2003. Desalination 152, 133.
Juttner, K., Manadhar, K., Seifer-Kraus, V., Loranz, W.J., 1986. Werkst Schmidt Korr. 37, 377.
Juttner, K., Loranz, W.J., Kending, M.W., Mansfeld, F., 1988. J. Electrochem. Soc. 135, 335.
Kendig, M., Jeanjaquet, S., 2002. J. Electrochem. Soc. 149, B47.
Khaled, K.F., 2008. Mater. Chem. Phys. 112, 290.
Khaled, K.F., 2008. Mater. Chem. Phys. 112, 104–111.
Khaled, K.F., 2008. Electrochim. Acta 53, 3484.
Khaled, K.F., 2009. J. Solid Stat. Eectrochem. 13, 1743.
Kutej, P., Vosta, J., Bartos, M., 1995. In: Proc. Eighth Eur. Symp. Corros. Inhibitors (8SEIC), Ann. Univ. Ferrara, Italy 10, p. 896.
Lee, H.P., Nobe, K., 1986. J. Electrochem. Soc. 133, 2035.
Lukovits, I., Kalman, E., Baka, I., Felhasi, I., Teledgi, J., 1995. In: Proc. Eighth Eur. Symp. Corros. Inhibitors (8SEIC), Ann. Univ. Ferrara, Italy 10, p. 543.
Lukovits, I., Kostalanyi, T., Kalman, E., Palinkos, G., 1999. Conference Corrosion 99, San Antonia, TX, USA, p. 565.
Lukovits, I., Kalman, E., Zucchi, F., 2001. Corrosion 57, 3.
Ma, H., Chen, S., Niu, L., Zhao, S., Li, S., Li, D., 2002. J. Appl. Electrochem. 32, 65.
Mansfeld, F., Wang, Y., 1995. In: Corrosion 95 NACE, Paper, No. 41.
McCafferty, E., 2005. Corros. Sci. 47, 3202.
McMahon, A.J., Harrop, D., 1995. In: Corrosion 95 NACE, Paper No. 32.
Mineva, T., Parvanov, V., Petrov, I., Neshev, N., Russo, N., 2001. J. Phys. Chem. A 105, 1959.
Pajkossy, T., 1994. J. Electroanal. Chem. 364, 111.
Pearson, R.G., 1986. Proc. Nat. Acad. Sci. 83, 8440.
Pearson, R.G., 1988. Inorg. Chem. 27, 734.
Qu, J., Guo, X., Chen, Z., 2005. Mater. Chem. Phys. 93, 388.
Raicheva, S.N., Sokolova, E.I., Zlateva, D.S., 1980. In: Proceedings of Fourth European Symp. Corrosion Inhibitors, Ferrara, Italy, p. 755.
Ram, V.J., Berche, D.A.V., Vlietinck, A.J., 1984. J. Heterocycl. Chem. 21, 1307.
Rosales, B., Vera, R., Moriena, G., 1999. Corros. Sci. 41, 625.
Saleh, R.M., Abd El-Alim, M.A., Hosary, A.A., 1983. Corrosion Prevention and Control February 9, p. 19.
Sherif, E.M., 2006. J. Appl. Surf. Sci. 252, 8615.
Sherif, E.M., Park, S.-M., 2005. J. Electrochem. Soc. 152, B428.
Sherif, E.M., Park, S.-M., 2006. Corros. Sci. 48, 4065.
Singh, M.M., Rastogi, R.B., Upadhyay, B.N., Yadav, M., 2003. Mater. Chem. Phys. 80, 283.
Speckmann, H.D., Strehblow, H.H., 1984. Werkst Korros. 35, 512.
Van Muydler, J., 1981. In: Bockris, J'.O.M., Conway, B.E., Yeager, E., White, R.E. (Eds.), Comprehensive Treatise of Electrochemistry, vol. 4. Plenum Press, New York, pp. 1–96.
Vera, R., Layana, G., Gardiazabal, J.I., 1995. Bol. Soc. Chil. Quím. 40, 149.
Vosta, J., Eliasek, J., 1971. Corros. Sci. 11, 223.
Wang, C., Chen, S., Zhao, S., 2004. J. Electrochem. Soc. 151, B11.
Zhao, P., Liang, Q., Li, Y., 2005. Appl. Surf. Sci. 252, 1596.